

Investigation of CO₂ Capture Ability in Amino Acid Ionic Liquid-Functionalized Metal-organic Frameworks

Chang YANG^{1*}, Kai LI², Yuan SU³, Yiwen LI⁴

¹ Wenzhou Municipal Motor Vehicle Exhaust Pollution Prevention and Control Management Center, Wenzhou 325000, Zhejiang, China

² Wenzhou Ecological and Environmental Monitoring Center of Zhejiang Province, Wenzhou 325000, Zhejiang, China

³ Wenzhou Institute of Eco-environmental Science, Wenzhou 325000, Zhejiang, China

⁴ Wenzhou Ecological and Environmental Promotion Center, Wenzhou 325000, Zhejiang, China

<http://doi.org/10.5755/j02.ms.40688>

Received 6 March 2025; accepted 6 May 2025

Due to their significant porosity and adjustable structures, metal-organic frameworks (MOFs) exhibit great promise for CO₂ sequestration. This investigation focuses on the augmentation of CO₂ capture capabilities in MOF-177 through impregnation with two amino acid-derived ionic liquids (AAILs), [BMIm]Glu and [BMIm]Asn. The AAIL@MOF-177 composites obtained were analyzed, confirming successful AAIL loading without significant disruption of the MOF structure. Remarkably, the composites demonstrated a marked enhancement in CO₂ uptake and preference for CO₂/N₂ and CO₂/CH₄ relative to the pristine MOF-177, especially under low-pressure conditions typical of post-combustion flue gas. The optimal AAIL loading was determined to be 30 wt.%. Under conditions of 0.2 bar and 25 °C, [BMIm]Asn-30@MOF-177 achieved a CO₂ uptake of 0.48 mmol/g, a 3.5-fold increase over pristine MOF-177. Furthermore, [BMIm]Asn-30@MOF-177 demonstrated superior CO₂/N₂ and CO₂/CH₄ selectivities of 14.2 and 11.9, respectively, under 0.2 bar and 35 °C. This enhanced performance arises from the robust chemical affinity between CO₂ and the amino groups in the AAIL anions, especially the two amino groups in [BMIm]Asn. The composites also showed excellent reusability over multiple adsorption-desorption cycles. These findings demonstrate the promising potential of AAIL-functionalized MOFs for efficient CO₂ capture.

Keywords: CO₂ capture, metal-organic frameworks, ionic liquids, amino acid ionic liquids, MOF-177.

1. INTRODUCTION

According to the "2023 Global Carbon Emissions Report" published by the International Energy Agency (IEA) in March 2024, global CO₂ emissions related to energy reached 37.4 billion tons in 2023, a 1.1 % increase over 2022, setting a new historical high. Excessive CO₂ emissions exacerbate the greenhouse effect, leading to global warming, glacier melting, rising sea levels, and other related issues. In addition, the flue gas from coal-fired power plants also contains a large amount of CO₂ and typically exhibits high temperatures, which increases the difficulty of CO₂ adsorption and removal. Overall, the current situation of CO₂ pollution is severe, and global efforts are needed to reduce emissions and strengthen control measures to address the environmental challenges it presents [1, 2].

Common methods for CO₂ recovery and capture include absorption and adsorption techniques [3–5], with absorption being a mature technology that is widely applicable, stable, and operationally reliable [3–6]. Traditional CO₂ chemical absorbents are typically organic amine solvents, such as monoethanolamine, diethanolamine, and methyldiethanolamine. Amino acid ionic liquids (AAILs), which have low melting points, good thermal stability, and low viscosity, are environmentally friendly, biocompatible, and biodegradable, making them a

new type of green solvent [7, 8]. In particular, AAILs demonstrate excellent performance in enhancing CO₂ absorption efficiency and cyclic stability, offering broad application prospects. Compared with traditional organic amine absorbents, AAILs are more efficient, have low regeneration energy consumption, and can achieve resource-efficient and green CO₂ recycling, making them promising for widespread industrial application. However, solvent absorption methods can cause issues such as corrosion, significant energy loss, and high costs during use, which affect their practical application. In contrast, solid porous materials have advantages in CO₂ adsorption, such as high adsorption efficiency, easy recovery, convenient operation, and good material stability, making solid-phase adsorption a growing research focus.

Metal-organic frameworks (MOFs), renowned for their expansive surface areas and customizable pore architectures, can significantly enhance CO₂ adsorption when loaded with ionic liquids [9–11]. Systematically studying the interaction mechanisms between MOFs and ionic liquids provides a theoretical foundation for selecting appropriate MOF systems to host ionic liquids, further promoting their application in CO₂ capture. Therefore, in this study, MOF-177 was synthesized via a solvothermal method, and amino acid ionic liquids were loaded onto MOF-177 using an impregnation method to prepare composite adsorbents (AAILs@MOF-177) for CO₂

* Corresponding author: C. Yang
E-mail: ChangYang@WZ.govr.org.cn

adsorption and separation. The physicochemical properties of the materials were studied using XRD, FT-IR, BET, and other methods. Adsorption isotherms were conducted across pressures from 0.1 to 1.0 bar and at temperatures of 25 °C, 35 °C, and 45 °C. The CO₂/N₂ and CO₂/CH₄ adsorption selectivity were also evaluated, along with an investigation into the underlying adsorption processes.

2. MATERIALS AND METHODS

2.1. Chemical reagents

[BMIm]Glu and [BMIm]Asn were acquired from Mernie Chemical Technology (Shanghai) Co., Ltd., with a purity > 98 %. N,N-Dimethylformamide, 1,3,5-Tris(4-carboxyphenyl)benzene, zinc nitrate hexahydrate, and methanol were acquired from Sigma-Aldrich and are of analytical grade. These substances were employed in their original state, without extra purification. Beijing Huanyu Jinghui Jingcheng Gas Technology Co., Ltd. supplied CO₂, CH₄, and N₂ with a purity of 99.99 %.

2.2. Material processing

2.2.1 Synthesis of MOF-177

MOF-177 was produced by means of a solvothermal method. A solution was made by dissolving 160 mg of 1,3,5-Tris(4-carboxyphenyl)benzene and 2400 mg of zinc nitrate hexahydrate in 48 mL of N,N-dimethylformamide (DMF). The resulting mixture was sonicated for 1 hour to promote dissolution. The solution was sealed in a heat-resistant glass tube and subjected to 85 °C for 3500 minutes. After cooling, the mixture was filtered and washed at least three times with DMF. Afterward, it was rinsed three times with toluene to eliminate impurities, resulting in yellow crystalline MOF-177. Prior to adsorption experiments, overnight drying of MOF-177 was conducted at 110 °C.

2.2.2 Fabrication of AAIL@MOF-177 composites

Amino acid ionic liquids [BMIm]Glu and [BMIm]Asn were loaded onto the porous MOF-177 support via an impregnation method using methanol as the solvent. The specific procedure is as follows: A certain amount of AAIL was introduced into a small glass bottle, which held 4 mL of methanol, then shaken for 30 minutes to ensure uniform mixing. A predetermined amount of dried MOF-177 was then added to another glass bottle, and the AAIL-methanol solution was added dropwise while stirring for 1 hour. The mixture was subsequently rotated at ambient temperature under reduced pressure for 24 hours to evaporate the solvent. The next step involved drying the composite at 80 °C for 2 hours to get rid of any leftover solvent. Prepared composite specimens were placed inside a glove box purged with argon to avoid moisture uptake and were designated as AAILs-X@MOF-177, where X denotes the weight percentage of AAIL. For example, the composite containing 15 wt.% [BMIm]Glu was labeled as [BMIm]Glu-15@MOF-177.

2.3. Material characterization

The chemical groups present in the specimens were characterized by FTIR (Thermo Fisher Scientific Nicolet

iS20, USA), spanning from 4000–400 cm⁻¹. The specimens' crystalline structures were assessed with XRD (Bruker D8 Advance, Germany), utilizing a 2θ range between 5° and 80°. The diffraction utilized copper as the source, with settings of 45 kV for acceleration voltage and 40 mA for current, and a scan rate of 0.01° per second. The thermal stability of [BMIm]Glu, [BMIm]Asn, pure MOF-177, and the composite materials AAILs@MOF-177 was analyzed using a Thermogravimetric Analyzer (HITACHI STA200, Japan) under a nitrogen stream of 50 mL/min and a temperature escalation of 10 °C/min from ambient temperature to 800 °C. Roughly 10 mg of the specimen was employed for every analysis. The specific surface area and pore capacity of pure MOF-177 and AAILs@MOF-177 were determined using a Micromeritics ASAP 2460 automatic surface area and porosity analyzer (USA) through N₂ adsorption and desorption isotherms.

2.4. Adsorption isotherms

Data on CO₂ adsorption were collected at 25 °C, 35 °C, and 45 °C under pressure conditions from 0.1 to 1.0 bar, and N₂ and CH₄ adsorption data were measured at 35 °C. A fully automated gravimetric analyzer, consisting of a computer-controlled microbalance with a precision of 1 μg, was used to measure the adsorption isotherms. Approximately 50–70 mg of adsorbent was introduced into the specimen vial. The specimen chamber was heated to 80 °C using a water bath, and after the system was vacuum-pumped to 10 mbar using a diaphragm and turbine pump, the specimen weight remained constant for 1 hour, indicating the removal of solvents, moisture, and impurities. After the degassing process, the water bath temperature was adjusted to the predetermined isothermal temperature, and the specimen was allowed to reach equilibrium at the set temperature. Once the specimen was prepared, the gas pressure was adjusted to 0.1 to 1.0 bar, and the isotherm measurement began. To ensure the desired pressure, the CO₂, CH₄, or N₂ flow into the chamber was regulated by a mass flow controller. The mass, temperature, and pressure of the adsorption system were monitored in real-time. After 2 hours of reaction under the set pressure, the results were recorded, and the next isotherm experiment was conducted.

2.5. Cycling

Based on the aforementioned adsorption isotherm experimental procedure, [BMIm]Glu-30@MOF-177 and [BMIm]Asn-30@MOF-177 were used to adsorb CO₂ at 30 °C. When adsorption became saturated, the CO₂ gas flow was halted, and the column was flushed with N₂ for 30 minutes to eliminate any remaining CO₂. After desorption, the column use for adsorption was brought back to ambient temperature, and the experiment was repeated to assess the adsorbent's performance over multiple cycles. The capacity for adsorption in each cycle was noted.

3. RESULTS AND DISCUSSION

3.1. Material characterization

Fig. 1 demonstrates the XRD characterization of the crystal structure of both pure MOF-177 and AAIL-loaded MOF-177 composites. The XRD pattern of MOF-177

exhibited distinctive peaks at $2\theta = 5.5^\circ, 5.8^\circ, 6.0^\circ, 6.2^\circ, 7.7^\circ, 10.5^\circ,$ and 11.3° , aligning closely with the literature data [12], confirming the structural integrity of the pristine MOF. For the AAIL/MOF-177 composites, the principal distinctive peaks of MOF-177 remained observable, implying that the crystallinity of MOF-177 was not destroyed after AAIL incorporation. However, slight shifts in peak positions and changes in the relative intensities were observed, suggesting a modification in the electronic environment within the crystal structure. This alteration was probably caused by AAIL occupying the MOF-177 pores, which resulted in alterations to the electronic structure or atomic orientations within the crystal lattice.

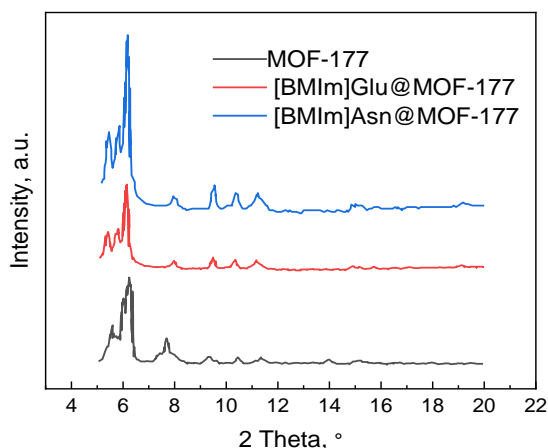


Fig. 1. XRD patterns of MOF-177 and AAIL/MOF-177 composites

Fig. 2 displays the FTIR spectra of pure AAIL, MOF-177, and AAIL/MOF-177 composites. For pure AAIL, a stretching vibration of $-\text{CH}_2-$ and $-\text{CH}_3$ in the imidazole ring was observed at 2935 cm^{-1} . The bending vibrations for C-H and C=N within the imidazole ring were detected at 1056.3 cm^{-1} and 753.1 cm^{-1} , respectively, confirming the presence of the imidazole structure. Peaks at 3147.7 cm^{-1} and 3076.4 cm^{-1} , attributed to N-H stretching vibrations, indicate an $-\text{NH}_2$ group is present. The carbonyl (C=O) and hydroxyl (O-H) stretching vibrations were detected at 1560.1 cm^{-1} and 2874.4 cm^{-1} , indicating a carboxyl group in the AAIL structure. For the pristine MOF-177, characteristic peaks at 511 cm^{-1} and 1596 cm^{-1} were observed, which were associated with the Zn-O and O-C-O groups of BTB, respectively. After loading AAIL into MOF-177, the Zn-O peak shifted from 511 cm^{-1} to 480 cm^{-1} , hinting at a diminished strength of the Zn-O bond, which is indicative of interactions between the AAIL cations and the Zn-O bonds within the MOF's porous structure.

Thermal stability of the materials was evaluated by conducting tests with thermogravimetric analysis (Tg). As shown in Fig. 3, the thermal degradation behavior of pure [BMIm]Glu and [BMIm]Asn exhibited a sharp weight loss at temperatures above 200°C , indicating rapid thermal decomposition. The decomposition onset temperatures of [BMIm]Glu and [BMIm]Asn were approximately 210°C and 220°C , respectively, whereas the pure MOF-177 exhibited significantly higher thermal stability with an onset decomposition temperature of approximately 420°C , consistent with previous literature [13]. For AAIL@MOF-

177 composites, a slight weight loss of 2–4 wt.% was observed below 75°C , which is likely due to residual methanol from the synthesis process.

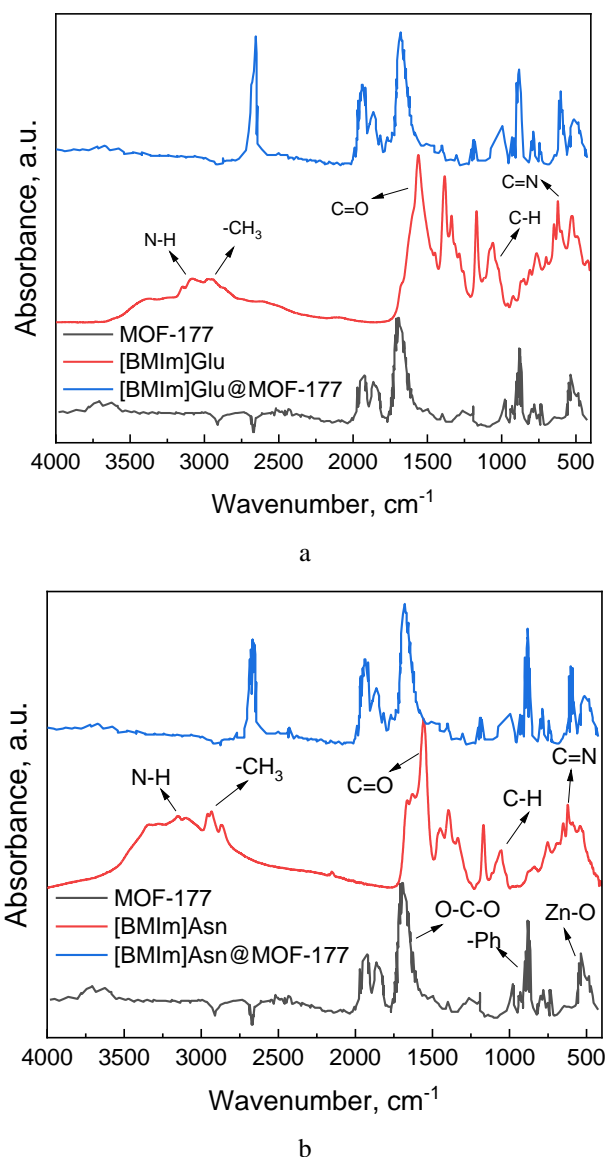


Fig. 2. FTIR spectra of MOF-177, AAIL, and AAIL/MOF-177 composites: a – [BMIm]Glu composites; b – [BMIm]Asn composites

Notably, the AAIL components in the composites underwent gradual decomposition between 250°C and 300°C before the MOF-177 decomposition began. This progressive degradation behavior was more pronounced in composites with higher AAIL loadings, such as [BMIm]Glu-45@MOF-177 and [BMIm]Asn-45@MOF-177, indicating surface interactions between AAIL and MOF-177.

To examine how AAIL loading influences the surface area and pore structure of MOF-177, nitrogen (N_2) adsorption-desorption isotherms were measured at 77 K (Fig. 4). A BET surface area of $4213\text{ m}^2\cdot\text{g}^{-1}$ was determined for unadulterated MOF-177, matching values found in the literature [14]. In contrast, AAIL@MOF-177 composites demonstrated a notable reduction in N_2 adsorption capacity relative to pure MOF-177, indicating that AAIL loading substantially reduces both the surface area and pore volume

of MOF-177. Specifically, the BET surface areas of the composites containing 15 wt.% [BMIm]Glu and [BMIm]Asn were reduced to $264 \text{ m}^2 \cdot \text{g}^{-1}$ and $197 \text{ m}^2 \cdot \text{g}^{-1}$, respectively.

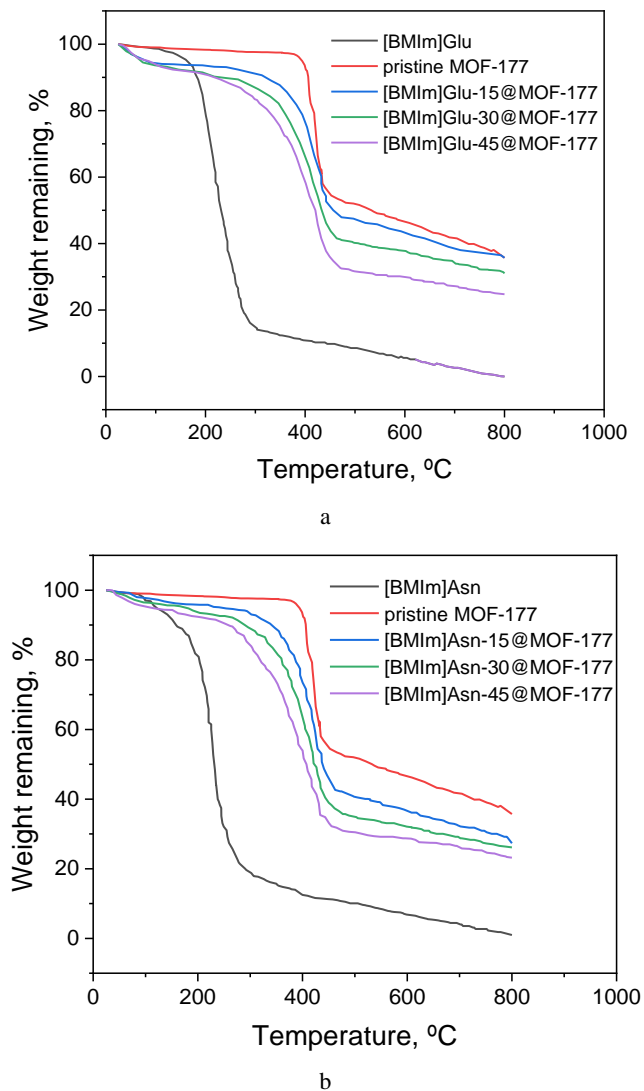


Fig. 3. Tg curves of AAIL, MOF-177, and AAIL@MOF-177 composites: a–[BMIm]Glu composites; b–[BMIm]Asn composites

As the AAIL loading increased, both surface area and pore volume continued to decrease, with [BMIm]Glu-45@MOF-177 showing a marked reduction in surface area ($32 \text{ m}^2 \cdot \text{g}^{-1}$) and pore volume ($0.03 \text{ cm}^3 \cdot \text{g}^{-1}$). Notably, [BMIm]Glu@MOF-177 exhibited a slightly higher surface area and pore volume compared to [BMIm]Asn@MOF-177, likely due to differences in molecular structure and the nature of interactions between the AAILs and MOF-177. Therefore, it can be concluded that AAIL molecules occupy the pores of MOF-177, leading to pore blockage and, consequently, a decline in N_2 adsorption capability. Higher AAIL loading raises the likelihood of pore blockage, thereby further hindering the N_2 adsorption performance of the composite material. These findings suggest that higher AAIL loading is not necessarily beneficial, and a careful, balanced evaluation of loading levels is essential to optimize material performance.

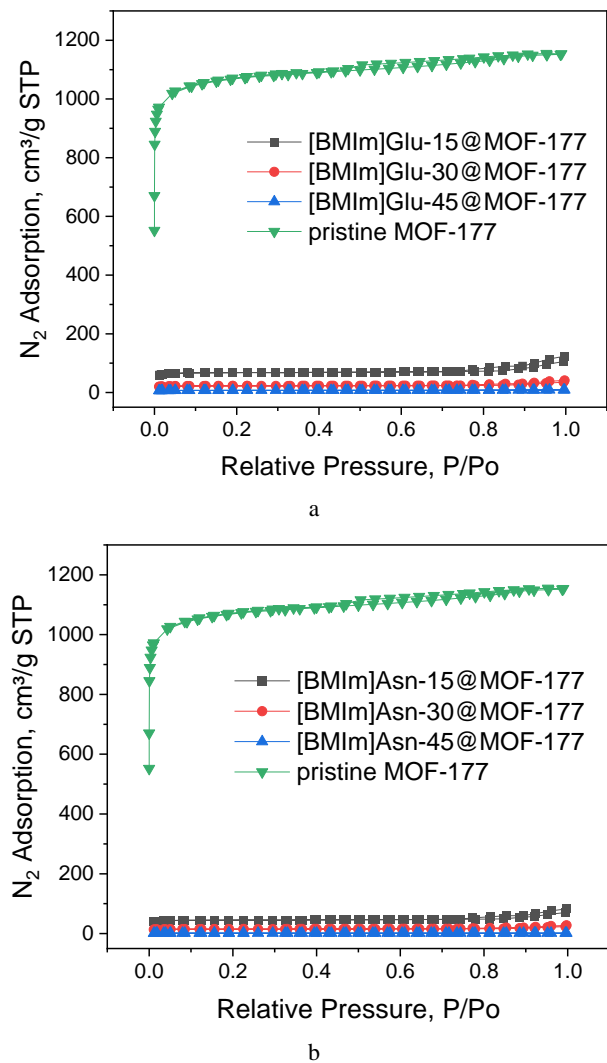


Fig. 4. N_2 adsorption-desorption isotherms at 77 K of pure MOF-177 and AAIL@MOF-177 composites: a–[BMIm]Glu composites; b–[BMIm]Asn composites

3.2. CO_2 capture performance of the adsorbent

Owing to the porous properties of MOF-177, it exhibits strong CO_2 adsorptive potential. However, its CO_2 adsorption performance is quite low under excessive combustion conditions (up to 0.15 bar) [15]. Therefore, in this study, [BMIm]Glu and [BMIm]Asn were used to modify MOF-177, resulting in [BMIm]Glu@MOF-177 and [BMIm]Asn@MOF-177 composites, which were then used for CO_2 capture. The equilibrium CO_2 uptake of these composites were measured under pressures of 0.1 to 1.0 bar at 25 °C, 35 °C, and 45 °C. Fig. 5 shows the equilibrium CO_2 adsorption of unadulterated MOF-177 and [BMIm]Asn@MOF-177 composites over the 0.1 to 1.0 bar pressure range.

Incorporation of [BMIm]Asn into MOF-177 boosted its ability to capture CO_2 under low-pressure conditions (0.1 to 1.0 bar). Relative to pure MOF-177, CO_2 uptake rose considerably with AAIL addition, achieving its highest level at 30 wt.% loading. At 0.2 bar and 25 °C, [BMIm]Asn-30@MOF-177 captured 0.48 mmol/g of CO_2 , which is about 3.5 times higher than the adsorption of pure MOF-177 under the same conditions. However, increasing the AAIL loading to 45 wt.% did not result in a significant increase in

CO₂ adsorption. On the contrary, compared to the composite with 30 wt% loading, the CO₂ uptake decreased to 0.32 mmol/g, which is only slightly higher than that of pure MOF-177 under the same conditions. When the temperature increased from 25 °C to 35 °C and 45 °C, the CO₂ adsorption capacity of the composites decreased at the same pressure.

It should be noted that the composite material with 15 wt.% AAILs shows higher CO₂ adsorption capacity than the original MOF-177 when the pressure is below 0.8 bar, but slightly lower capacity at 1.0 bar. This is because the composite material mainly relies on chemical interactions between the amino groups on AAILs and CO₂, while the original MOF-177 adsorbs CO₂ primarily through physical interactions, which are more significantly influenced by pressure.

Fig. 6 illustrates the equilibrium CO₂ adsorption for unadulterated MOF-177 and [BMIm]Glu@MOF-177 over the 0.1 to 1.0 bar pressure range. MOF-177's capacity to adsorb CO₂ was improved by the inclusion of [BMIm]Glu, consistent with the results for [BMIm]Asn@MOF-177 composites. The composite [BMIm]Glu-30@MOF-177 showed superior CO₂ capture performance compared to all other [BMIm]Glu@MOF-177 composites and pure MOF-177. This composite adsorbed 0.34 mmol/g of CO₂ at 0.2 bar and 25 °C, nearly 2.5 times the amount adsorbed by pure MOF-177 in identical circumstances. As the [BMIm]Glu loading rose to 45 wt.%, the CO₂ capture capacity decreased. Notably, at the same temperature and pressure, [BMIm]Glu@MOF-177 composites showed lower CO₂ adsorption than [BMIm]Asn@MOF-177 composites when the AAIL loadings were identical. This is mainly due to the fact that the anion of [BMIm]Asn contains two amino groups, while the anion of [BMIm]Glu contains only one, making [BMIm]Asn more effective in binding to CO₂, leading to higher adsorption capacity.

3.3. Selectivity of the adsorbent

To evaluate the effectiveness of the AAIL@MOF-177 composites in capturing CO₂ from natural gas and post-combustion flue gas, the selectivity of the solid adsorbent towards CO₂ was compared with nitrogen (N₂) and methane (CH₄). Therefore, CO₂/N₂ and CO₂/CH₄ selectivities were determined by evaluating the adsorption isotherms of N₂ and CH₄ at 35 °C across a pressure span from 0.1 to 1.0 bar. In this study, to calculate selectivity, the molar adsorption amounts of each component were compared at a particular pressure, with the formulas for CO₂/N₂ and CO₂/CH₄ selectivities shown in Eq. 1 and Eq. 2.

$$S_{CO_2/N_2} = \frac{q_{CO_2}}{q_{N_2}}; \quad (1)$$

$$S_{CO_2/CH_4} = \frac{q_{CO_2}}{q_{CH_4}}, \quad (2)$$

where, S_{CO_2/N_2} and S_{CO_2/CH_4} represent the selectivity of CO₂/N₂ and CO₂/CH₄, respectively, while q_{CO_2} , q_{N_2} , and

q_{CH_4} correspond to the molar adsorption amounts of CO₂, N₂, and CH₄, respectively.

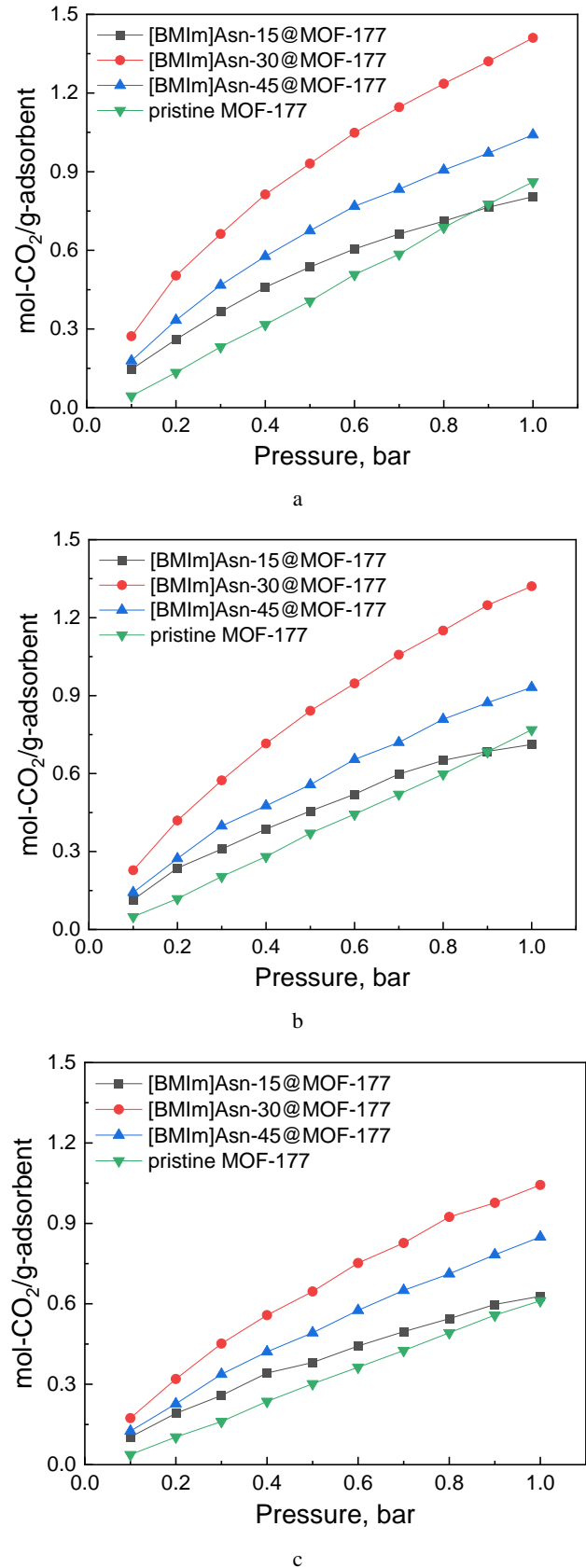
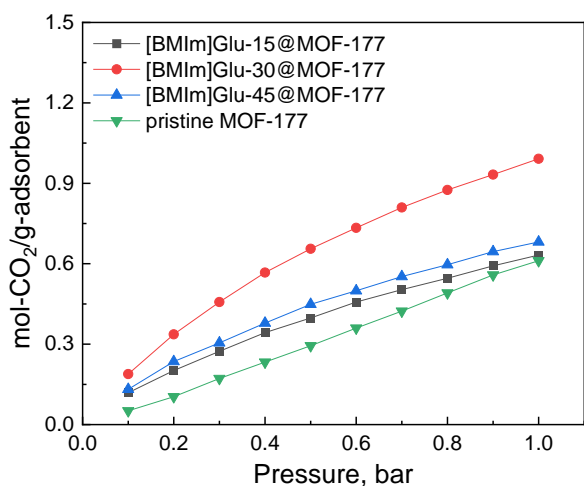
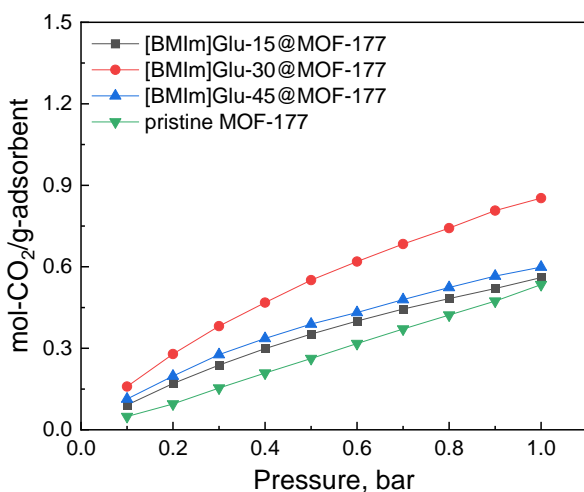


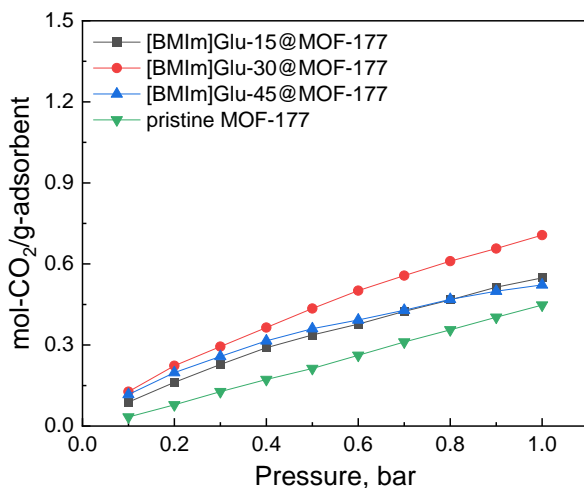
Fig. 5. Equilibrium CO₂ adsorption capacity of [BMIm]Asn@MOF-177 composite at 0.1-1.0 bar pressure range at different temperatures: a-25 °C; b-35 °C; c-45 °C



a



b

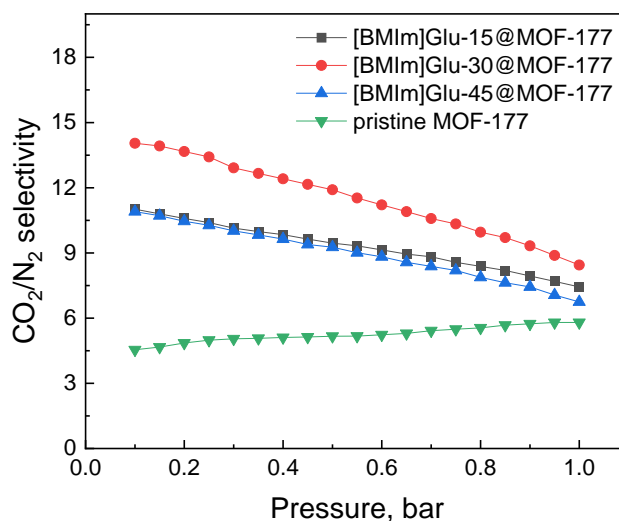


c

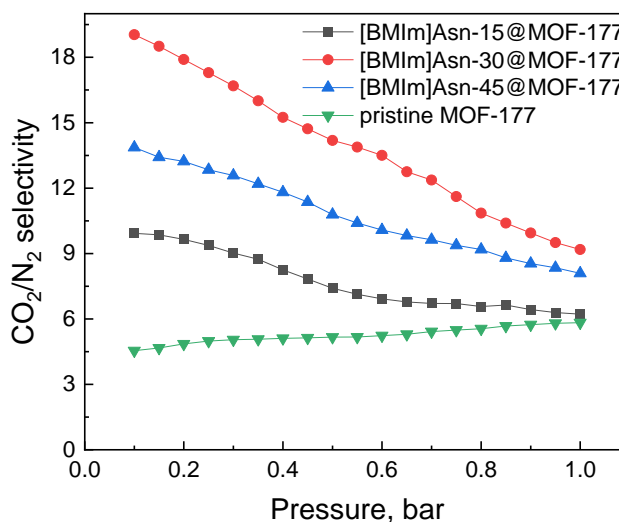
Fig. 6. Equilibrium CO₂ adsorption capacity of [BMIm]Glu@MOF-177 composite at 0.1–1.0 bar pressure range at different temperatures: a–25 °C; b–35 °C; c–45 °C

Fig. 7 illustrates the CO₂/N₂ and CO₂/CH₄ selectivity calculations for the [BMIm]Glu@MOF-177 and [BMIm]Asn@MOF-177 composites. In the pressure range of 0.1 to 1.0 bar, the CO₂/N₂ and CO₂/CH₄ selectivities of pure MOF-177 fluctuated between 3 and 5. When [BMIm]Glu and [BMIm]Asn were incorporated into MOF-

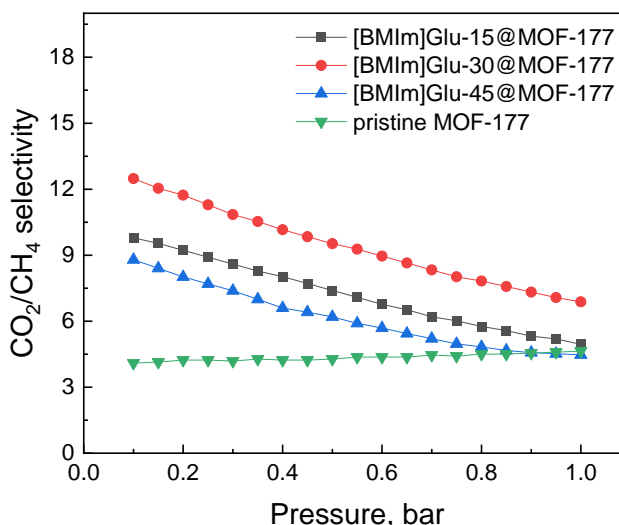
177, the CO₂/N₂ and CO₂/CH₄ selectivities of the AAIL@MOF-177 composites were significantly enhanced compared to pure MOF-177.



a



b



c

continued on next page

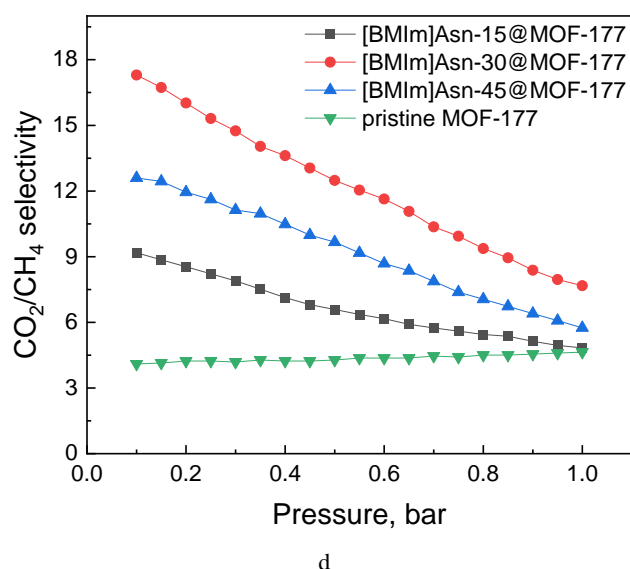


Fig. 7. CO₂/N₂ and CO₂/CH₄ selectivity of the composites: a–CO₂/N₂ selectivity of [BMIm]Glu@MOF-177; b–CO₂/N₂ selectivity of [BMIm]Asn@MOF-177; c–CO₂/CH₄ selectivity of [BMIm]Glu@MOF-177; d–CO₂/CH₄ selectivity of [BMIm]Asn@MOF-177

Specifically, [BMIm]Glu-30@MOF-177 exhibited the highest CO₂/N₂ and CO₂/CH₄ selectivities, reaching 14.2 and 11.9 at 0.2 bar and 35 °C, respectively. Notably, increasing the [BMIm]Glu loading from 30 wt.% to 45 wt.% did not result in further improvement in selectivity. A comparable trend was noted for the [BMIm]Asn@MOF-177 composites, where [BMIm]Asn-30@MOF-177 demonstrated the best CO₂/N₂ and CO₂/CH₄ selectivities. Furthermore, the CO₂/N₂ and CO₂/CH₄ selectivities of [BMIm]Glu@MOF-177 were lower than those of [BMIm]Asn@MOF-177, which can be attributed to the stronger CO₂ adsorption performance of [BMIm]Asn. However, for all AAIL@MOF-177 composites, it was observed that the CO₂/N₂ and CO₂/CH₄ selectivities gradually decreased as the pressure increased. It should be noted that the CO₂/N₂ and CO₂/CH₄ selectivities of the original MOF-177 increase with increasing pressure mainly because the adsorption of CO₂, N₂, and CH₄ on MOF-177 is dominated by physical interactions. Differences in gas molecule sizes, available adsorption sites, and interaction strengths contribute to stronger CO₂ adsorption at higher pressures, thereby enhancing the selectivity toward CO₂.

3.4. Reusability of the adsorbent

Reusability is one of the most important factors for industrial applications. Therefore, the reusability of the adsorbent was analyzed, and the outcomes are depicted in Fig. 8. After 5 adsorption-desorption cycles, both [BMIm]Glu-30@MOF-177 and [BMIm]Asn-30@MOF-177 composites maintained excellent CO₂ adsorption performance. The stable performance confirms that these AAIL composites possess good reusability and can be recycled for practical applications.

3.5. Discussion

The robust interaction between CO₂ and the amino group in AAILs significantly enhances the CO₂ capture of

MOF-177 when modified with AAIL. Previous studies have shown that the reaction between CO₂ and the amino groups in AAIL is similar to the dissolution process of amines in water [16].

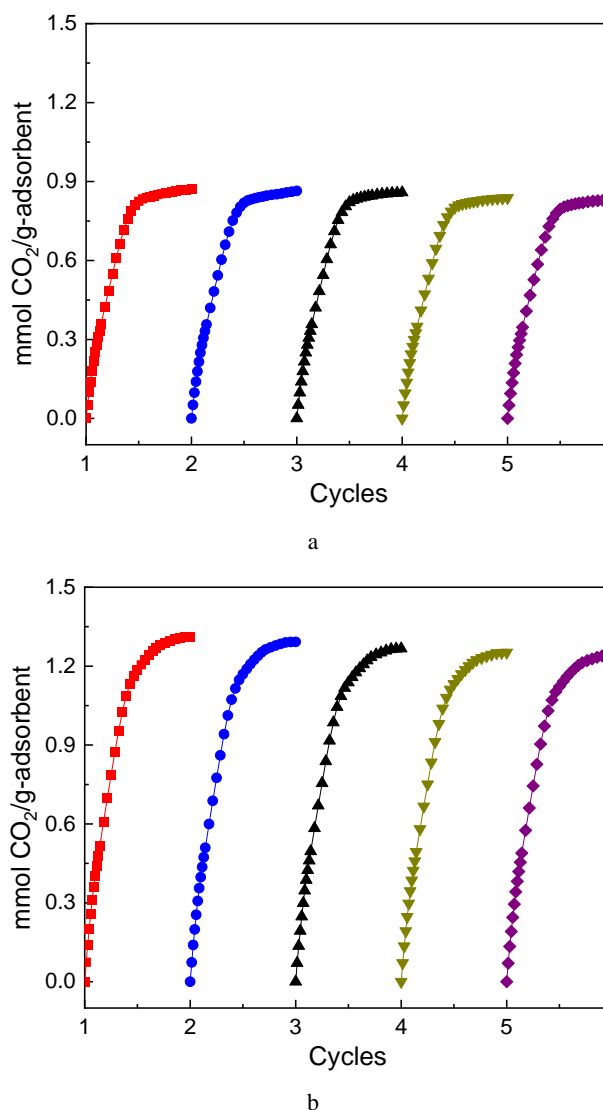


Fig. 8. Reusability of [BMIm]Glu-30@MOF-177 and [BMIm]Asn-30@MOF-177 composites after 5 cycles of adsorption-desorption: a–[BMIm]Glu-30@MOF-177 composites; b–[BMIm]Asn-30@MOF-177 composites

Wang et al. [17] proposed that CO₂ can approach the amino groups in the amino acid anion of [Emim][Gly] and react to form a carbamate with a 2:1 molar ratio. Similarly, in composite materials, amino groups also interact with CO₂ to create carbamate, enhancing CO₂ capture capacity more than unadulterated MOF-177 within the 0.1–1.0 bar pressure range. Notably, at pressures ranging from 0.1 to 1.0 bar, the CO₂ capture in the composite materials is dominated by chemical adsorption due to the strong affinity between CO₂ and AAIL, leading to improved CO₂ uptake. On the other hand, the AAIL molecules occupy the pore channels of MOF-177, which significantly reduces the pore volume and surface area of the composite materials. As the pressure increases, physical adsorption becomes dominant in CO₂ capture, apart from the active chemical adsorption sites. As surface area plays a crucial role in physical adsorption, the

advantage of the composite materials in CO₂ capture gradually diminishes, and their CO₂ adsorption may even fall below that of pure MOF-177.

Moreover, the AAIL loading amount also influences the CO₂ adsorption capacity of the composite materials. However, it's essential to acknowledge that the CO₂ uptake does not continuously increase with higher AAIL loading. In this study, an ideal AAIL loading of 30 wt.% was identified. When the loading exceeded this threshold, composite materials experienced a decline in their capacity to adsorb CO₂. The decline in the ability to adsorb CO₂ is attributed to the clogging of the pores in the host material, which reduces the number of accessible adsorption sites. Evidence for this is also provided by the BET surface area and pore volume measurements for the AAIL-loaded MOF-177 composites with a 45 wt.% loading. Wang et al. [17] impregnated [Emim][Gly] into the nanoporosity of polymethyl methacrylate (PMMA) and applied it for CO₂ capture. They found that when the loading of [Emim][Gly] increased from 0 wt.% to 100 wt.%, the optimal loading was 50 wt.%. Similarly, Uehara et al. [18] loaded [Emim][Lys] onto mesoporous silica (SBA-15) and observed a similar trend, with the optimal loading being 60 wt.%.

The introduction of AAILs to MOF-177 enhances the CO₂/N₂ and CO₂/CH₄ adsorption selectivity. Previous studies suggest that the amino acid anions form active chemical adsorption sites, which increase the affinity for CO₂ and promote the formation of N-C bonds. After loading the amino acid ionic liquids onto MOF-177, the surface area and pore volume decrease, but the CO₂ adsorption capacity of the composite material still increases, resulting in improved selectivity. Additionally, N₂ and CH₄ show no affinity for the amino groups. Because their adsorption is primarily physical, the adsorption amount depends mainly on surface area. Therefore, compared to N₂ and CH₄ absorption, CO₂ adsorption dominates at low pressures, leading to higher CO₂/N₂ and CO₂/CH₄ selectivity. However, increasing pressure highlights the importance of physical adsorption sites in addition to active chemical sites in impacting adsorption capacity. Consequently, with higher pressure, the composites exhibit lower selectivity for CO₂/N₂ and CO₂/CH₄.

4. CONCLUSIONS

This investigation proved that incorporating [BMIm]Glu and [BMIm]Asn amino acid ionic liquids into MOF-177 enhanced its CO₂ capture performance and selectivity. The AAIL@MOF-177 composites exhibited significantly higher CO₂ uptake compared to pristine MOF-177, particularly at low pressures. An optimal AAIL loading of 30 wt.% was identified, beyond which pore blockage led to a decrease in performance. Specifically, [BMIm]Asn-30@MOF-177 showed a 3.5-fold increase in CO₂ uptake (0.48 mmol/g at 0.2 bar and 25 °C) and superior CO₂/N₂ (14.2) and CO₂/CH₄ (11.9) selectivities (at 0.2 bar and 35 °C) compared to both pristine MOF-177 and the [BMIm]Glu-loaded counterpart. This enhancement is attributed to the robust chemisorption of CO₂ by the amino groups in the AAILs, with the two amino groups in [BMIm]Asn providing a greater advantage. The composites also demonstrated excellent recyclability.

While this study highlights the significant potential of AAIL@MOF-177 composites, further investigations are warranted. Future work should focus on: (1) exploring a wider range of AAILs with varying structures and functionalities to optimize the CO₂ capture performance; (2) conducting detailed computational studies to elucidate the specific interaction mechanisms between CO₂ and the AAILs at the molecular level; and (3) assessing the durability and effectiveness of these materials in actual flue gas environments over an extended period, including the presence of moisture and other trace components. To fully evaluate the practicality of deploying this technology in large-scale CO₂ capture operations, further studies focusing on scale-up are essential.

REFERENCES

1. **Nunes, L.J.** The Rising Threat of Atmospheric CO₂: A Review on the Causes, Impacts, and Mitigation Strategies *Environments* 10 (4) 2023: pp. 66. <https://doi.org/10.3390/environments10040066>
2. **Zhang, L., Wang, Q., Zhang, M.** Environmental Regulation and CO₂ Emissions: Based on Strategic Interaction of Environmental Governance *Ecological Complexity* 45 2021: pp. 100893. <https://doi.org/10.1016/j.ecocom.2020.100893>
3. **Ochedi, F.O., Yu, J., Yu, H., Liu, Y., Hussain, A.** Carbon Dioxide Capture Using Liquid Absorption Methods: A Review *Environmental Chemistry Letters* 19 2021: pp. 77–109. <https://doi.org/10.1007/s10311-020-01093-8>
4. **Soo, X.Y.D., Lee, J.J.C., Wu, W.Y., Tao, L., Wang, C., Zhu, Q., Bu, J.** Advancements in CO₂ Capture by Absorption and Adsorption: A Comprehensive Review *Journal of CO₂ Utilization* 81 2024: pp. 102727. <https://doi.org/10.1016/j.jcou.2024.102727>
5. **Yoro, K.O., Daramola, M.O., Sekoai, P.T., Armah, E.K., Wilson, U.N.** Advances and Emerging Techniques for Energy Recovery During Absorptive CO₂ Capture: A Review of Process and Non-Process Integration-Based Strategies *Renewable and Sustainable Energy Reviews* 147 2021: pp. 111241. <https://doi.org/10.1016/j.rser.2021.111241>
6. **Raganati, F., Ammendola, P.** CO₂ Post-Combustion Capture: A Critical Review of Current Technologies and Future Directions *Energy & Fuels* 38 (15) 2024: pp. 13858–13905. <https://doi.org/10.1021/acs.energyfuels.4c02513>
7. **Guncheva, M., Yakimova, B.** Diversity of Potential (Bio) Technological Applications of Amino Acid-Based Ionic Liquids *Applied Sciences* 15 (3) 2025: pp. 1515. <https://doi.org/10.3390/app15031515>
8. **Fan, J.P., Yuan, C., Lai, X.H., Xie, C.F., Chen, H.P., Peng, H.L.** Density, Viscosity and Electrical Conductivity of Four Amino Acid Based Ionic Liquids Derived from L-Histidine, L-Lysine, L-Serine, and Glycine *Journal of Molecular Liquids* 364 2022: pp. 119944. <https://doi.org/10.1016/j.molliq.2022.119944>
9. **Li, X., Chen, K., Guo, R., Wei, Z.** Ionic Liquids Functionalized Mofs for Adsorption *Chemical Reviews* 123 (16) 2023: pp. 10432–10467. <https://doi.org/10.1021/acs.chemrev.3c00248>
10. **Chafiq, M., Fatimah, S., Chaouiki, A., Ko, Y.G.** Synergistic Sorption Strategies: Ionic Liquids-Modified Mof

Matrices for Adsorption Processes *Separation and Purification Technology* 2024: pp. 128056.
<https://doi.org/10.1016/j.seppur.2024.128056>

11. **Ali, S.A., Khan, A.U., Mulk, W.U., Khan, H., Nasir Shah, S., Zahid, A., Habib, K., Shah, M.U.H., Othman, M.H.D., Rahman, S.** An Ongoing Futuristic Career of Metal–Organic Frameworks and Ionic Liquids, a Magical Gateway to Capture CO₂; a Critical Review *Energy & Fuels* 37 (20) 2023: pp. 15394–15428.
<https://doi.org/10.1021/acs.energyfuels.3c02377>
12. **Tranchemontagne, D.J., Hunt, J.R., Yaghi, O.M.** Room Temperature Synthesis of Metal–Organic Frameworks: Mof-5, Mof-74, Mof-177, Mof-199, and Irmof-0 *Tetrahedron* 64 (36) 2008: pp. 8553–8557.
<https://doi.org/10.1016/j.tet.2008.06.036>
13. **Mohamedali, M., Henni, A., Ibrahim, H.** Investigation of CO₂ Capture Using Acetate-Based Ionic Liquids Incorporated into Exceptionally Porous Metal–Organic Frameworks *Adsorption* 25 2019: pp. 675–692.
<https://doi.org/10.1007/s10450-019-00073-x>
14. **Furukawa, H., Miller, M.A., Yaghi, O.M.** Independent Verification of the Saturation Hydrogen Uptake in Mof-177 and Establishment of a Benchmark for Hydrogen Adsorption in Metal–Organic Frameworks *Journal of Materials Chemistry* 17 (30) 2007: pp. 3197–3204.
<https://doi.org/10.1039/B703608F>
15. **Liu, R.S., Shi, X.D., Wang, C.T., Gao, Y.Z., Xu, S., Hao, G.P., Chen, S., Lu, A.H.** Advances in Post-Combustion CO₂ Capture by Physical Adsorption: From Materials Innovation to Separation Practice *ChemSusChem* 14 (6) 2021: pp. 1428–1471.
<https://doi.org/10.1002/cssc.202002677>
16. **Ren, J., Wu, L., Li, B.G.** Preparation and CO₂ Sorption/Desorption of N-(3-Aminopropyl) Aminoethyl Tributylphosphonium Amino Acid Salt Ionic Liquids Supported into Porous Silica Particles *Industrial & engineering chemistry research* 51 (23) 2012: pp. 7901–7909.
<https://doi.org/10.1021/ie2028415>
17. **Wang, X., Akhmedov, N.G., Duan, Y., Luebke, D., Li, B.** Immobilization of Amino Acid Ionic Liquids into Nanoporous Microspheres as Robust Sorbents for CO₂ Capture *Journal of Materials Chemistry A* 1 (9) 2013: pp. 2978–2982.
<https://doi.org/10.1039/C3TA00768E>
18. **Uehara, Y., Karami, D., Mahinpey, N.** CO₂ Adsorption Using Amino Acid Ionic Liquid-Impregnated Mesoporous Silica Sorbents with Different Textural Properties *Microporous and Mesoporous Materials* 278 2019: pp. 378–386.
<https://doi.org/10.1016/j.micromeso.2019.01.011>



© Yang et al. 2026 Open Access This article is distributed under the terms of the Creative Commons Attribution 4.0 International License (<http://creativecommons.org/licenses/by/4.0/>), which permits unrestricted use, distribution, and reproduction in any medium, provided you give appropriate credit to the original author(s) and the source, provide a link to the Creative Commons license, and indicate if changes were made.